https://doi.org/10.5194/egusphere-2026-5916
Preprint. Discussion started: 9 November 2026
© Author(s) 2026. CC BY 4.0 License.

Retrieval of surface NO_2 from Pandora direct sun measurements

Darby Bates[1], Ramina Alwarda[1], Xiaoyi Zhao[2], Sum Chi Lee[2], Debora Griffin[3], Yushan Su[4], Alexander Cede[5], Kimberly Strong[1]

[1]Department of Physics, University of Toronto, Toronto, ON, M5S 1A7, Canada
[2]Atmospheric Composition Monitoring Division, Environment and Climate Change Canada, Toronto, ON, M3H 5T4, Canada
[3]Earth Systems Research and Integration Division, Environment and Climate Change Canada, Toronto, ON, M3H 5T4, Canada
[4]Ontario Ministry of the Environment, Conservation, and Parks, Toronto, ON, M9P 3V6, Canada
[5]LuftBlick, Innsbruck, Austria, and NASA/GSFC Code 614, Greenbelt, MD, USA

Correspondence to: Darby Bates (darby.bates@mail.utoronto.ca)

Abstract. Nitrogen dioxide (NO_2), a criteria pollutant used for the Air Quality Health Index (AQHI) reporting, can have important environmental and human respiratory health effects when present in the near-surface atmosphere. For this study, urban surface volume mixing ratios (VMRs) are derived from Pandora total column measurements. Pandora remote sensing instruments can be used to evaluate surface air quality and complement in situ instruments to support long-term monitoring of ambient air quality. At four sites in the Greater Toronto Area and Detroit-Windsor Area, Pandora direct sun measurements are converted to surface VMRs following a method utilizing a high-resolution air quality forecasting model. The resulting VMRs agree with coincident in situ measurements to within 2 ppbv from 2020 through 2024. This method is shown to be most effective when the Planetary Boundary Layer (PBL) is above 750 m as estimated by ERA5 reanalysis, while dependence on PBL height below 750 m is evaluated. The surface VMR derived from Pandora direct sun measurements when the PBL is below 750 m has a median difference of -1.7 ppbv (parts per billion by volume) (10^{th} percentile: -8.2 ppbv, 90^{th} percentile: 3.2 ppbv) with respect to coincident in situ measurements. When a logarithmic correction is applied as a function of PBL height for these shallow PBL conditions, the median difference is reduced to 0.5 ppbv (-4.8 ppbv, 4.1 ppbv).

1 Introduction

Pollutants in the near-surface atmosphere can adversely affect human and environmental health. Nitrogen dioxide (NO_2) is a criteria pollutant used for the Air Quality Health Index (AQHI) that is commonly emitted by anthropogenic sources (Siu et al., 2025) and that can harm human

https://doi.org/10.5194/egusphere-2026-5916
Preprint. Discussion started: 9 November 2026
© Author(s) 2026. CC BY 4.0 License.

respiratory health directly and indirectly. NO_2 exposure itself can lead to respiratory problems, and nitrogen oxides ($NO_x = NO + NO_2$) in the atmosphere contribute to the formation of surface ozone that can also damage lung tissue (Lamsal et al., 2015). The 2025 Canadian Ambient Air Quality Standards for NO_2 specify outdoor air quality objectives of 42 ppbv (parts per billion by volume) for the one-hour metric and 12 ppbv for the annual metric (Canadian Council of Ministers of the Environment, 2025).

To quantify this exposure, ambient surface NO_2 concentrations are monitored using in situ gas analyzer instruments. The National Air Pollution Surveillance (NAPS) program in Canada and the Air Quality System (AQS) program of the US Environmental Protection Agency in the United States constitute expansive networks of in situ instruments that have been used to monitor NO_2 concentrations and trends (Lamsal et al., 2015) and to evaluate remote-sensing measurements of NO_2, including from TEMPO and TROPOMI (Siu et al., 2025) in North America.

The remote-sensing ground-based Pandora UV-visible spectrometers that comprise the Pandonia Global Network (PGN) can measure atmospheric composition using multiple viewing geometries, including Multi-AXis Differential Optical Absorption Spectroscopy (MAX-DOAS), zenith-sky, and direct sun (DS) measurements, from which total column, partial column, and vertical profile NO_2 products are retrieved (Cede, 2024). These PGN L2 products have been used to track NO_2 concentrations during the COVID-19 pandemic (Zhao et al., 2022) in the Toronto area, to assess air quality improvement via NO_2 near-surface concentration reduction in Rome from 2017 through 2022 (Di Bernardino et al., 2023), and to validate satellite data. OMI satellite column retrievals alongside surface observations showed modest correlation to Pandora (Lamsal et al., 2014), while TROPOMI, with its smaller pixel size, showed better agreement (Judd et al., 2020; Verhoelst et al., 2021; Park et al., 2022). The goal of this study is to derive NO_2 surface volume mixing ratios (VMRs) from Pandora direct sun total columns.

We present NO_2 surface VMRs derived from Pandora total column measurements by applying the high-resolution air quality forecast model-based conversion method from Zhao et al. (2019). To convert from total columns to surface VMRs, the method uses: (i) the ratio of NO_2 surface volume mixing ratio to planetary boundary layer column from the Environment and Climate Change Canada (ECCC) regional air quality forecast model called Global Environmental Multi-scale-Modelling Air quality and Chemistry (GEM-MACH), (ii) the stratospheric NO_2 column from the Pandora, and (iii) the free tropospheric NO_2 column from the Goddard Earth

https://doi.org/10.5194/egusphere-2026-5916
Preprint. Discussion started: 9 November 2026
© Author(s) 2026. CC BY 4.0 License.

Observing System-Chemistry (GEOS-Chem) chemical transport model. Using this method, Zhao et al. (2019) showed that the surface VMRs derived from Pandora zenith-sky total columns agreed to within ±2 ppbv when compared with in situ measurements in Toronto at the Downsview site from 2015 to 2017.

This study evaluates the effectiveness of this algorithm when applied to total columns from Pandora direct sun measurements at four sites in Toronto and in the Detroit-Windsor Area under different meteorological and pollutant conditions. These sites include Downsview and Toronto West in the Greater Toronto Area (GTA) as well as Southwest (SW) Detroit and Windsor West in the Detroit-Windsor Area (DWA), shown on the maps in Fig. 1. To investigate how well the derived surface estimates capture surface NO_2 behaviour, the VMRs derived from Pandora direct sun total NO_2 columns are compared to measurements made by in situ instruments at each site as a function of time and of meteorological conditions. A new correction method is developed and verified to improve the results in low Planetary Boundary Layer (PBL) height conditions.

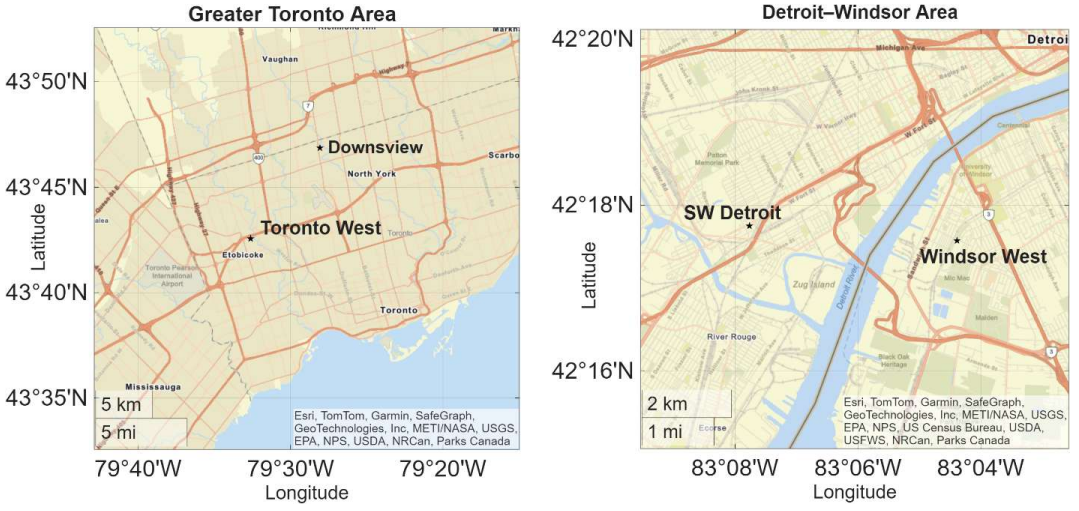


Figure 1. Maps of Pandora sites showing Downsview and Toronto West in the Greater Toronto Area (left) and SW Detroit and Windsor West in the Detroit-Windsor Area (right), with each site marked with a black star. Maps were created using the MathWorks MATLAB Mapping Toolbox. Powered by Esri. Image source: (left) Esri, TomTom, Garmin, SafeGraph, GeoTechnologies, Inc, METI/NASA, USGS, EPA, NPS, USDA, NRCan, Parks Canada (right) Esri, TomTom, Garmin, SafeGraph, GeoTechnologies, Inc, METI/NASA, USGS, EPA, NPS, US Census Bureau, USDA, USFWS, NRCan, Parks Canada.

This paper is organized as follows. Section 2 presents the datasets used in this work. Section 3 provides an overview of the column-to-surface conversion method. Section 4 summarizes results for each site with respect to time of day and season, and summarizes the impact of meteorological conditions, including wind speed and direction, and PBL height, on the

https://doi.org/10.5194/egusphere-2026-5916
Preprint. Discussion started: 9 November 2026
© Author(s) 2026. CC BY 4.0 License.

agreement between the derived VMR estimates and in situ VMR measurements for each site. Finally, Section 5 summarizes the outcomes of this study.

2 Datasets and models

In this study, NO_2 columns retrieved from remote-sensing measurements are combined with atmospheric model outputs to derive surface NO_2 VMRs that are evaluated against nearby in situ measurements. The datasets used in this study comprise three categories: measurements by in situ instruments, retrievals from remote sensing instruments, and outputs from atmospheric models.

To derive surface NO_2 VMRs from column measurements of NO_2 following the method used in this study, at least three datasets are required as inputs. Each site is described in Section 2.1, then each dataset is described in Sections 2.2 to 2.4. Table 1 summarizes the datasets that serve as inputs for the conversion method of Zhao et al. (2019), described in detail in Section 3.

Table 1. Instrument name, site coordinates, datasets, and period covered in this work.

	Instrument	Site (Lat, Lon)	Datasets	Period
Remote sensing	Pandora 104	Downsview, ON, Canada (43.7810, -79.4680)	NO_2 total columns from Direct Sun observations, climatological NO_2 stratospheric columns	2020-2024
	Pandora 108	Toronto West, ON, Canada (43.7094, -79.5435)		2021-2024
	Pandora 208	Windsor West, ON, Canada (42.2929, -83.0731)		2022-2024
	Pandora 147	SW Detroit, MI, USA (42.3026, -83.1068)		2021-2024
Model	GEOS-Chem	Selected to nearest grid box to each Pandora location	NO_2 free tropospheric columns	2020-2024
	GEM-MACH		NO_2 surface VMRs, NO_2 PBL columns	
	ERA-5		Planetary Boundary Layer (PBL) height, zonal and meridional winds on pressure levels averaged on lowest five levels from 1000-900 Pa, 10 m temperature	
In situ	Thermo Fisher 42i (MECP & NAPS)	Downsview (43.7805, -79.4674) Toronto West (43.7094, -79.5435) Windsor-West	NO_2 surface observations	2020-2024 2021-2024 2022-2024

https://doi.org/10.5194/egusphere-2026-5916
Preprint. Discussion started: 9 November 2026
© Author(s) 2026. CC BY 4.0 License.

		(42.2929, -83.0731)		
	Thermo Fisher 42i (EGLE & EPA/AQS)	SW Detroit (42.3028, -83.1062)		2021-2024

2.1 In situ measurements

Section 2.1.1 describes the two sites in the Greater Toronto Area and Section 2.1.2 describes the two sites in the Detroit-Windsor Area. Each site hosts an in situ NO_x analyzer that measures NO_2 surface VMRs with hourly resolution, operated by the Ontario Ministry of the Environment, Conservation, and Parks (MECP) as part of the National Air Pollution Surveillance (NAPS) program in Canada and by the Department of Environment, Great Lakes, and Energy (EGLE) as part of the AQS program in the United States.

In situ NO_2 concentrations were indirectly measured using a Thermo Fisher 42i NO-NO_2-NO_x analyzer based on the chemiluminescence technology. This method may overestimate NO_2 due to interference from other reactive nitrogen species (e.g., nitric acid and peroxyacetyl nitrate), particularly in areas with limited direct emissions of nitrogen oxides (e.g., rural areas). To evaluate this potential bias, co-located measurements were conducted from 2016 to 2022 at the Downsview site and the Highway 401 Roadside station near the Toronto West site using both the Thermo 42i and an API T500U, which employs cavity attenuated phase shift (CAPS) spectroscopy technology. The differences between direct and indirect NO_2 measurements were small, with median differences of 1 ppbv (0.6 ± 1.1 ppbv) at the Downsview site (May 2016 to February 2017) and 0.5 ppbv (0.3 ± 1.8 ppbv) at the Highway 401 Roadside station (March 2017 to March 2022).

2.1.1 Greater Toronto Area

The MECP conducts in situ measurements of common air pollutants at stations across Ontario. The Downsview site is at the Environment and Climate Change Canada (ECCC) Toronto headquarters, in a suburban area in the northern part of the Greater Toronto Area where the nearest point sources are traffic on Highway 407, which runs east-west and is approximately 2 km north of the site at its closest point, and traffic on Dufferin Street about 180 m west of the site. Pandora 104 was operated here from 2013 to 2024. The Toronto West site is an air-quality monitoring station that hosts Pandora 169 operated by ECCC and an in situ NO-NO_2-NO_x analyzer operated

https://doi.org/10.5194/egusphere-2026-5916
Preprint. Discussion started: 9 November 2026
© Author(s) 2026. CC BY 4.0 License.

by MECP. This site is in an urban area 150 m south of Highway 401 and is about 6 km east of the Toronto Pearson International Airport (YYZ). Data from the in situ and Pandora instruments covered the period from 2020-2024 for Downsview and 2021-2024 for Toronto West.

2.1.2 Detroit-Windsor Area

The Windsor West site in Ontario, Canada, is an air-quality monitoring station that hosts Pandora 208 operated by ECCC and an in situ chemiluminescence NOx analyzer operated by MECP. The Southwest Detroit site in Michigan, USA, is an air-quality monitoring station that hosts Pandora 147 and an in situ NO-NO_2-NO_x analyzer operated by the United States Environmental Protection Agency (EPA). Data from the in situ and Pandora instruments covered the period from 2022-2024 for Windsor West and 2021-2024 for SW Detroit. Hourly in situ measurements with 0.4 ppbv precision are used in this study to evaluate the performance of the Pandora column-to-surface derivation results.

Zug Island is a large industrial site on an island in the Detroit River that emits NO_2 as part of the steel production process. This site is near to both the Windsor West and SW Detroit sites, which are both in urban areas.

2.2 Remote sensing measurements

2.2.1 Pandora direct sun total NO_2 column and climatological stratospheric NO_2 column

The Pandora instruments used in this study are summarized in Table 1. Pandora instruments measure spectra using an Avantes spectrometer with a back-thinned CCD detector to measure from 280 to 530 nm at 0.6 nm spectral resolution. Using pan-tilt motors to point the optical head light entrance for measurements, Pandora spectrometers can achieve multiple viewing geometries, including direct sun, MAX-DOAS, and zenith-sky configurations. Among these, only direct sun Pandora measurement data are used for this study, i.e. NO_2 total columns from L2 retrieval version rnvs3p1-8 that are publicly available on the PGN website. PGN L2 data have been processed using a standardized retrieval implemented by the LuftBlick team and described in (Cede, 2024). This involves fitting the spectra using total optical absorption spectroscopy techniques to estimate NO_2 columns using the BlickO retrieval software. For this product, the retrieval is done in the visible range and involves calculating slant columns and scaling them by

https://doi.org/10.5194/egusphere-2026-5916
Preprint. Discussion started: 9 November 2026
© Author(s) 2026. CC BY 4.0 License.

the inverse of airmass factor estimated from the geometry of the direct sun viewing angle. More details on this data product can be found in the PGN Readme File (Cede et al., 2025).

Pandora instruments that run the measurement routine recommended by the PGN have a typical direct sun measurement duration from 30 seconds to one minute, with one measurement about every 11 minutes because the instrument alternates between viewing geometry modes. L2 Pandora NO_2 columns from direct sun measurements come with detailed uncertainty information associated with each measurement point. The accuracies for cloud-screened data with up-to-date calibration typically range from 1 μmol/m^2 to 8 μmol/m^2 depending on solar zenith angle, as seen in Fig. 9 of Cede et al. (2025). The latest Pandora L2 rnvs3p1-8 data product includes climatological stratospheric NO_2 columns that can be used to estimate the stratospheric NO_2 column at the Pandora measurement time; these are derived from work done by Brohede et al. (2007). The impact (on the derived VMR, C_{pan}, in Eq. 1 below) of using Pandora climatological estimates rather than OMI stratospheric NO_2 columns was explored. This substitution was found to have no statistically significant impact on the agreement between the in situ and derived surface VMRs. In the rest of this study, stratospheric NO_2 column estimates at Pandora measurement times are the climatological values from rnvs3p1-8.

2.3 Atmospheric models

Two quantities are estimated from atmospheric model products: the free tropospheric NO_2 column; and the ratio of NO_2 surface VMR to PBL column. Several ERA5 reanalysis products are used to evaluate the performance of the Pandora column-to-surface conversion algorithm.

2.3.1 GEOS-Chem

The NASA Global Modelling and Assimilation Office's Goddard Earth Observing System (GEOS) meteorological observations are used as inputs to the GEOS-Chem atmospheric chemistry model. These are monthly concentrations from GEOS-Chem operational outputs on the 0.5° × 0.67° resolution grid, version v8-03-01 (Bey et al., 2001; McLinden et al., 2014). From these outputs, monthly mean NO_2 partial columns in the free-troposphere (1.5 to 12 km) were calculated to account for the fact that the GEM-MACH model does not currently include free tropospheric NO_2 sources. The free tropospheric NO_2 column estimates, for altitudes of 1.5 to 12 km defined to be the bounds of the free troposphere in GEOS-Chem, come from GEOS-Chem monthly averages

https://doi.org/10.5194/egusphere-2026-5916
Preprint. Discussion started: 9 November 2026
© Author(s) 2026. CC BY 4.0 License.

that have been interpolated to hourly time steps using the Pratmo box model (Brohede et al., 2008; Lindenmaier et al., 2011; McLinden et al., 2000). The PBL is considered to extend from the surface to 1.5 km in this estimate.

2.3.2 GEM-MACH

GEM-MACH is ECCC's operational regional air quality forecasting model (Moran et al., 2026a,b). Hourly surface pollutant concentrations over North America are generated twice daily for the next 48-hour period. The model is an extension of the ECCC Global Environmental Multi-scale (GEM) numerical weather prediction model with the addition of an online tropospheric chemistry module. Free-tropospheric NOx emissions from lightning and in-flight aircraft are not currently included in the operational GEM-MACH model, necessitating the use of GEOS-Chem estimates of free-tropospheric NO_2 in this study. Hourly NO_2 columns from 0 to 1.5 km and surface concentrations from archived operational forecasts on the native model grid over North America with 10 km × 10 km horizontal resolution for the period 2020 to 2024 have been gathered for this work. At each site in this study, the grid box located closest to the Pandora instrument was used. The ratio of surface VMR to PBL NO_2 column is estimated from the outputs of the operational version of GEM-MACH. At each site, the data from these models are selected from the grid box nearest to the site coordinates.

2.3.3 ERA5 reanalysis

ERA5 reanalysis products provide information about meteorological conditions at each site by selecting the model grid cell that contains the site. For this project, the ERA5 reanalysis products on single levels and on pressure levels are used. Wind u- and v- components on the lowest five pressure levels were downloaded (from 1000 hPa through 900 hPa in 250 hPa intervals). The u- and v- components were converted to wind direction and wind speed, and wind direction was sorted into 30° bins when evaluating the performance of the algorithm at each site. The PBL height was downloaded from the ERA5 reanalysis products on single levels and binned in 100 m high layers from 0 m at the surface to 2500 m, where PBL heights exceeding 2500 m were included in the last bin.

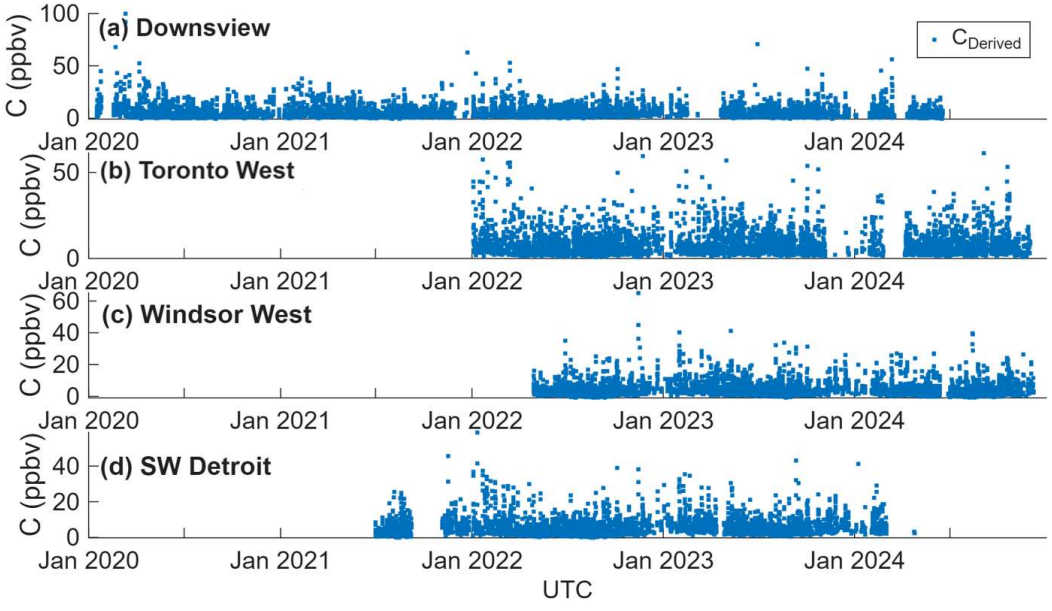
https://doi.org/10.5194/egusphere-2026-5916
Preprint. Discussion started: 9 November 2026
© Author(s) 2026. CC BY 4.0 License.

3 Column-to-surface conversion algorithm

Estimates of NO_2 surface VMR were derived from Pandora direct sun NO_2 total columns following the conversion method of Zhao et al. (2019). First, the stratospheric and free tropospheric NO_2 columns are subtracted from the total column to yield a planetary boundary layer NO_2 column, the first group of terms in parentheses in the equation below. Then, this PBL column is multiplied by the model ratio of VMR-to-PBL to estimate the NO_2 surface VMR. This method of converting Pandora direct sun NO_2 total column in Dobson units to surface VMR in ppbv follows:

$$C_{pan} = \left(V_{pan} - V_{strat} - V_{ftrop}\right) \times \left(\frac{C}{V_{PBL}}\right)_{G-M}, \quad (1)$$

where C_{pan} is the output derived NO_2 surface VMR, V_{pan} is the input Pandora direct sun total column NO_2, and the three additional inputs are the Pandora climatological stratospheric NO_2 column, V_{strat}; the GEOS-Chem free troposphere NO_2 column, V_{ftrop}, and the GEM-MACH ratio of surface VMR to PBL column NO_2, $\left(\frac{C}{V_{PBL}}\right)_{G-M}$. As the in situ and model outputs are reported hourly, the Pandora input is averaged hourly and therefore the C_{pan} are hourly. Figure 2 shows the resulting time series of C_{pan} at each site.



https://doi.org/10.5194/egusphere-2026-5916
Preprint. Discussion started: 9 November 2026
© Author(s) 2026. CC BY 4.0 License.

Figure 2. NO_2 surface VMR, $C_{Derived}$, derived from Pandora direct sun measurements at each site (in UTC). From top to bottom the panels show the time series of hourly measurements in ppbv at (a) Downsview, (b) Toronto West, (c) Windsor West, and (d) SW Detroit.

4 Results

4.1 Comparing derived VMR with in situ VMR

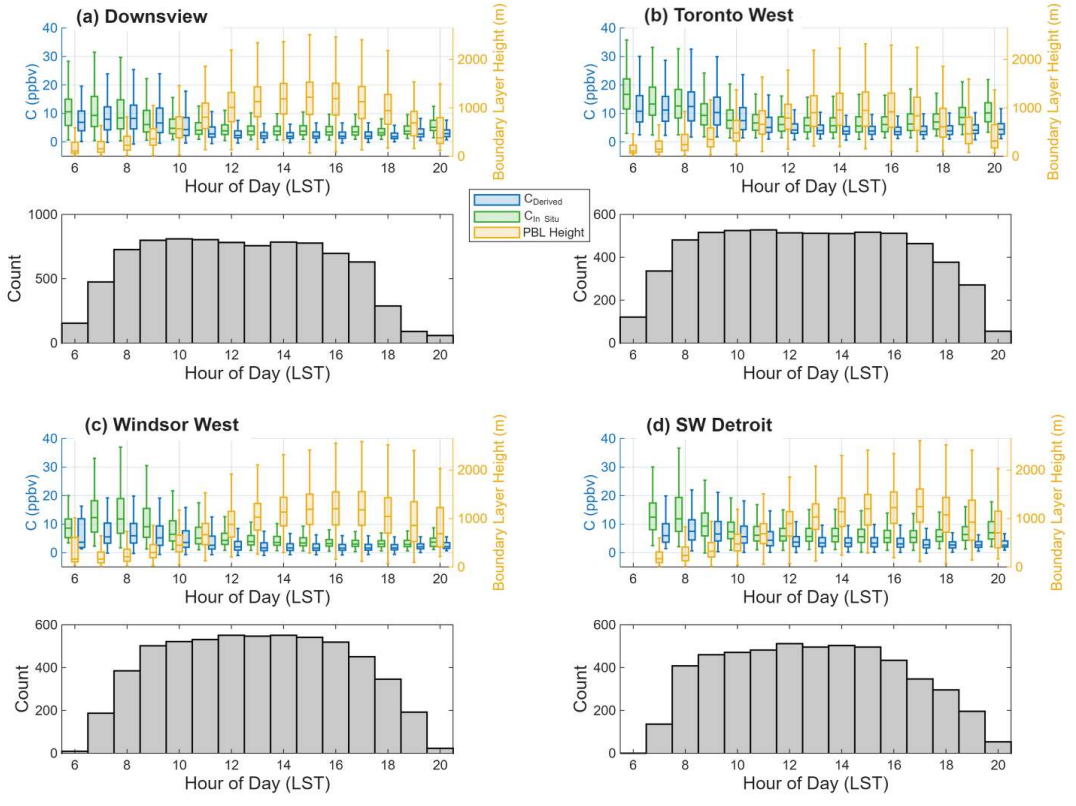
In urban environments, the NO_2 VMR near the surface during daylight hours (when direct sun measurements are made) tends to follow a diurnal pattern where NO_2 peaks early in the morning, around 7 AM local solar time (LST), then declines through the rest of the day into the evening. This is due to elevated emissions during traffic hours and low PBL heights in the early morning and may be less affected by photochemical processes that destroy NO_2. This expected time-of-day pattern in surface NO_2 is reflected in the in situ and the derived surface NO_2 VMRs, as shown in Fig. 3. The panels in Fig. 3 are comprised of dual y-axis hour-of-day box plots of surface VMR from in situ measurements and derived from Pandora measurements on the left axis and the PBL height on the right axis. Below those box plots are histograms of the counts of measurements during each daylight hour in the full time series at that site. Note that the Pandora direct sun measurements only take place when the sun is above the horizon, so there are no measurements before 7 AM LST and after 6 PM LST. In the morning around rush hour between 8 AM and 10 AM LST, both instruments tend to measure the peak surface NO_2 VMR. This coincides with the time of day when the PBL tends to be shallow as shown in orange. In the afternoon, NO_2 VMRs tend to decrease while the PBL height is on average higher than it is in the morning. The difference between the Pandora DS-derived and the in situ surface NO_2 VMRs is:

$$\Delta C = C_{pan} - C_{in\ situ}, \quad (2)$$

When ΔC is positive, the Pandora DS-derived surface VMR is larger than the in situ VMR. The hour of day difference between ΔC and PBL height are shown in Figure 4, no strong diurnal dependences of the agreement between the derived and in situ surface VMRs were found, but it can be noted that the largest values of ΔC appear to occur when the PBL height is shallow, below about 750 m, which tends to occur in the early morning and late evening. Figure 4 shows that measurement counts are much lower in the early morning and late evening, likely due to reduced or absent sunlight affecting Pandora observations. This raises the question of whether the accuracy and precision of Pandora measurements during these periods are comparable to those obtained

https://doi.org/10.5194/egusphere-2026-5916
Preprint. Discussion started: 9 November 2026
© Author(s) 2026. CC BY 4.0 License.

257 during the rest of the day; this along with undersampling could explain the larger ΔC values
258 observed. This shallow PBL height behaviour is discussed in the next section.
259



260

261 **Figure 3. The upper panel in each pair shows the hourly variation of $C_{In\ Situ}$ (green) and Pandora-derived (blue) NO_2 surface**
262 **VMR ($C_{Derived}$) along the left axis, and Planetary Boundary Layer height (PBL height) (yellow) along the right axis, at (a)**
263 **Downsview, (b) Toronto West, (c) Windsor West, and (d) SW Detroit. These box plots show the median and inter-quartile**
264 **range while the whiskers show the range of values excluding outliers. The lower panel in each pair shows coincident**
265 **measurement counts for both the Pandora and in situ instruments during each daylight hour for the full time series at each**
266 **site (hours when one or both of each pair of instruments lacked measurements have been excluded).**

267

https://doi.org/10.5194/egusphere-2026-5916
Preprint. Discussion started: 9 November 2026
© Author(s) 2026. CC BY 4.0 License.

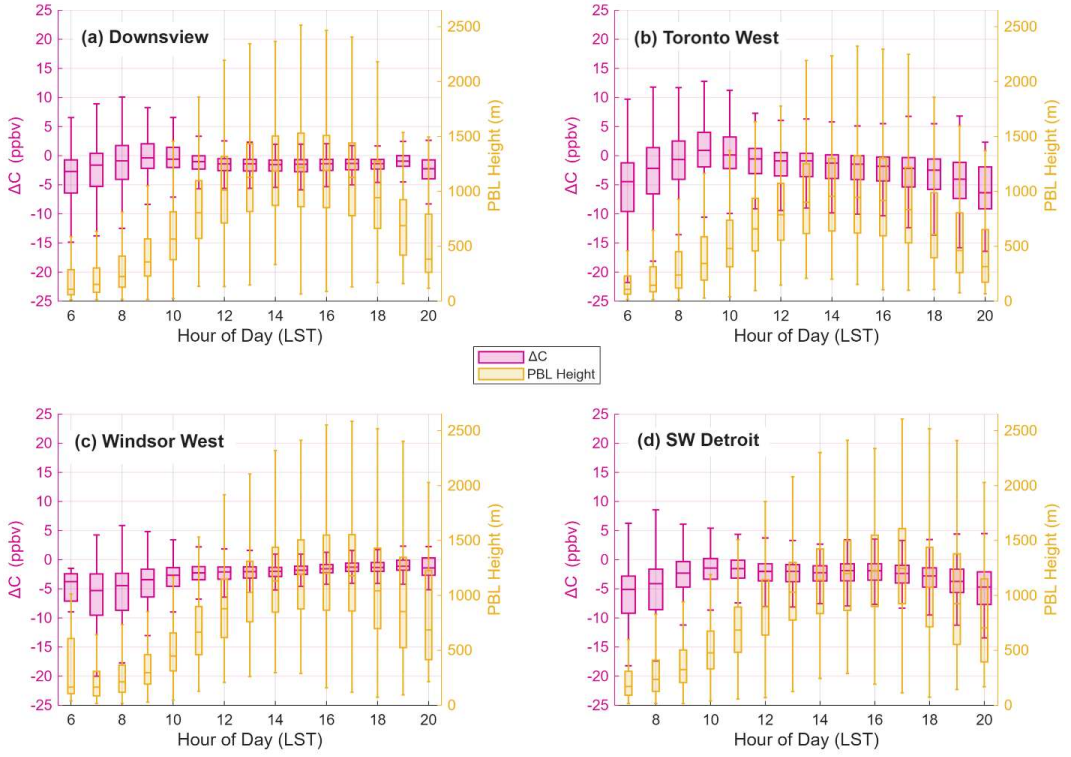


Figure 4. Hour of day variation of ΔC (ΔC = C_{pan} − $C_{in\ situ}$) (red) and PBL height (yellow) at (a) Downsview, (b) Toronto West, (c) Windsor West, and (d) SW Detroit. The box plots show the median and inter-quartile range while the whiskers show the range of values excluding outliers. When the PBL height is large, the differences tend to be closer to zero. For shallow PBL heights, however, ΔC shows larger deviations from zero in both the positive and negative direction, indicating that when the PBL height is shallow, the airmasses seen by the two instruments may be more different than when the PBL height is taller.

4.1.1 Boundary layer height dependence

The agreement between the derived C_{pan} and the in situ $C_{in\ situ}$ NO_2 surface VMR varies with PBL height. When the PBL height is above about 750 m, which constitutes at least 41% of the data at each site, this agreement appears to be independent of PBL height at Downsview, Windsor West, and SW Detroit. At Toronto West, in this regime the agreement still varies with PBL height, with maximum differences when PBL height is about 1500 m and better agreement for PBL heights above and below 1500 m. The Toronto West site is near Pearson International Airport and winds from the direction of the airport may be contributing to this different pattern, as even for higher PBL heights the mixing might not account for NO_2 from aircraft above.

https://doi.org/10.5194/egusphere-2026-5916
Preprint. Discussion started: 9 November 2026
© Author(s) 2026. CC BY 4.0 License.

In the regime where PBL height is below 750 m, the agreement improves with increasing PBL, as shown in Fig. 5. The median, 10th, and 90th percentile values of C_{pan}, $C_{in\ situ}$, and the difference ΔC when PBL height is below 750 m are presented in Table 2. When the PBL height is in this range, the NO_2 is less well-mixed, and the performance of the algorithm is expected to depend more strongly on NO_2 that is detected by the Pandora measurement and not by the in-situ measurement and might not be accounted for in the Pandora climatological stratospheric or GEOS-Chem free tropospheric NO_2 estimates. This NO_2 could come from local emission sources, including nearby traffic or local point sources. When the median ΔC is negative, the derived surface VMR often underestimates the in situ VMR, which occurs for Windsor West and SW Detroit, the two sites in urban areas with strong nearby point sources of NO_2. At Downsview, ΔC is smaller than at Windsor West or SW Detroit, which is likely due to the sites being in a more suburban area, with few nearby sources except one highway. At Toronto West, however, the small negative difference may be attributed to the Pandora instrument detecting lofted NO_2 that may come from airplanes approaching or departing the nearby Pearson International Airport that is about 6 km southwest of the site, since the site is often downwind of the airport. These plumes would pass through the Pandora measurement field-of-view without being transported to the surface when the PBL height is low and therefore mixing is limited and the surface instrument would give a better estimate of surface VMR under those conditions. SW Detroit and Windsor West have similar large negative median differences, which could be due to local emissions that are not detectable by the Pandora when the PBL height is shallow. It is possible that these changes in NO_2 are taking place outside of the direct sun cone, that is the field-of-view of the instrument in the direct sun viewing mode and might be detected by the local sensor without being seen by the Pandora.

Table 2. Median surface NO_2 volume mixing ratios from in situ measurements ($C_{in\ situ}$), Pandora DS-derived estimates (C_{pan}), and the difference between the two (ΔC) for PBL heights up to and including 750 m.

Site	Median $C_{in\ situ}$ (10th, 90th percentile) [ppbv]	Median C_{pan} (10th, 90th percentile) [ppbv]	Median ΔC (10th, 90th percentile) [ppbv]
Downsview	5.4 (1.6, 15.7)	6.3 (2.5, 19)	-1.2 (-7.1, 4.0)
Toronto-West	6.5 (2.6, 18.9)	8.0 (3.0, 19.4)	-0.6 (-7.4, 5.0)
Windsor West	3.9 (0.8, 12.7)	7.1 (2.3, 20)	-2.8 (-9.0, 0.0)
SW Detroit	5.7 (2.1, 14.4)	8.9 (3.8, 19.6)	-2.8 (-9.3, 1.6)

https://doi.org/10.5194/egusphere-2026-5916
Preprint. Discussion started: 9 November 2026
© Author(s) 2026. CC BY 4.0 License.

The agreement between the derived VMR and in situ VMR shows a logarithmic dependence on PBL height when PBL height is below 750 m at each site, as shown in Fig. 5. The relationship between NO_2 mixing and PBL height is such that with elevated PBL height, the surface NO_2 is approximately homogeneous, but when PBL height is shallow, the NO_2 near the surface is less well-mixed, which is approximately logarithmic in Fig. 5, especially at Windsor West and SW Detroit. Figures 3 and 4 support this claim that the air sampled by the Pandora spectrometer total column measurement is more similar to the air sampled by the in situ instrument when the PBL is high, as the spread of VMRs detected at different times of day in Fig. 3 is larger during times of day with lower PBL heights. The largest ΔC values in Fig. 4 occur primarily when the PBL height is very low. A proposed method to account for the dependence on PBL is described below.

This dependence can be fit using the following equation for all measurements for which the PBL height is below 750 m:

$$\Delta C = C_{pan} - C_{in\ situ} = a * \log(BLH) + b\ . \quad (2)$$

Here, BLH is the PBL height from ERA5, parameter a reflects the PBL height dependence of the difference between in situ and derived NO_2 VMR and is fit as one parameter across all sites, and parameter b reflects the offset due to horizontal or vertical separation between the in situ instrument and Pandora instrument at each site. This fitting is performed using the matrix fitting method with a non-linear regression model described below.

Data collected at all four sites are used to calculate a single shared parameter a, while data for each individual site are used to fit the site-specific parameter b, necessitating the application of a matrix fitting method, described in Appendix A. For this method, the inputs are three vectors and one indexing matrix. Hourly mean in situ and Pandora-derived surface VMRs and the ERA5 PBL height, represented by $\overrightarrow{C_{in\ situ}}$, $\overrightarrow{C_{pan}}$, and $\overrightarrow{BLH}$, respectively, are vectors that contain all the temporally coincident measurements at each site. Each of these three vectors has the same number of elements as there are coincident hourly measurements from the in situ and Pandora instruments across all sites in the study. An indexing matrix is applied such that the fit that results in scalar p_1 is calculated based on all measurements and vector $\vec{b}$ is composed of four b site-specific elements that are each calculated based only on the measurements at that site.

The resulting fits are shown in orange in Fig. 5, with fit parameters provided in Appendix A. The fits appear to match some of the variation with PBL heights between 0 and 750 m, but the

https://doi.org/10.5194/egusphere-2026-5916
Preprint. Discussion started: 9 November 2026
© Author(s) 2026. CC BY 4.0 License.

341 constraint that the parameter a remain the same across the sites is motivated by it being the
342 coefficient an offset due to vertical or horizontal displacement between the Pandora instrument
343 and the in situ instrument.

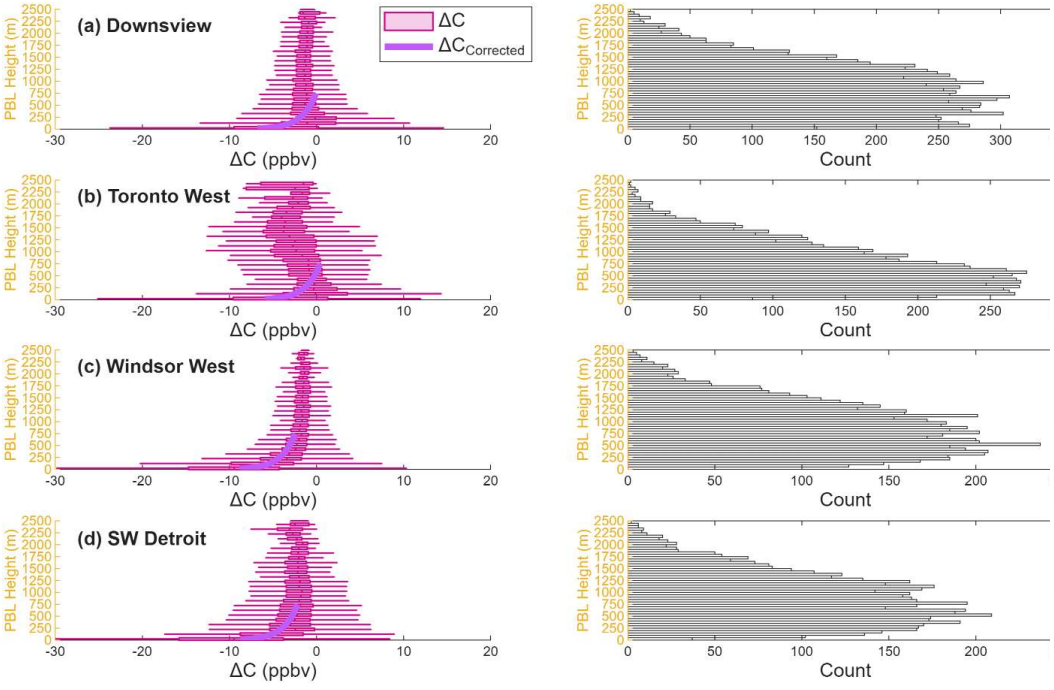


Figure 5. The left panel in each pair shows the variation of ΔC, the difference between Pandora-derived and in situ NO_2 surface VMR, with PBL height at (a) Downsview, (b) Toronto West, (c) Windsor West, and (d) SW Detroit. Each panel represents the data from a single site binned by PBL height in 100 m bins such that the lowest box plot represents measurements with PBL height from 0 to 100 m. The purple line, labelled $\Delta C_{Corrected}$, is the result of the logarithmic fit to account for the PBL height dependence of ΔC when the PBL height is below 750 m. The right panel in each pair shows the count of measurements in each 100 m PBL height bin.

344 **4.1.2 Time-of-day dependence**

345 Figure 6 shows the time-of-day variation of the difference between the derived and
346 corrected NO_2 surface VMRs relative to the in situ measurements when the PBL height is below
347 750 m. The differences are presented for two seasonal periods at each site: the warm season from
348 March through August in panels (a) through (d); and the cold season from September through
349 February in panels (e) through (h). While the derived surface NO_2 VMRs capture the behavior of
350 the in situ data over the course of the day, with a peak in the morning followed by a decrease
351 through midday, the time-of-day dependence of the agreement is not uniform across all sites.

https://doi.org/10.5194/egusphere-2026-5916
Preprint. Discussion started: 9 November 2026
© Author(s) 2026. CC BY 4.0 License.

The Windsor West, and Southwest Detroit sites are nearer to expected large sources of NO_2 including the Zug Island, a large industrial site point source to the south of SW Detroit and to the southwest of Windsor West. At these two sites, the derived surface VMR (blue) almost always underestimates the in situ VMR, while at Toronto West the derived surface VMR is sometimes overestimated and sometimes underestimated. The Toronto West site is near to Pearson International Airport, so this overestimation could be due to lofted NO_2 from planes coming to and departing from the airport when the PBL height is low, which tends to happen in the morning and evening. In the middle part of the day, the derived surface VMR underestimates the in situ VMR at Toronto West in the cold season, possibly because the PBL height tends to increase throughout the day and by evening the air is more well mixed, leading to possible underestimation of the surface VMR when derived using the method. The surface VMRs corrected for PBL height (orange) are in better agreement with the in situ estimates in the early morning, when the PBL height is low, suggesting that PBL height contributes to the underestimation. At Downsview and Toronto West, the correction is very small in the morning, but at SW Detroit and Windsor West the correction is larger.

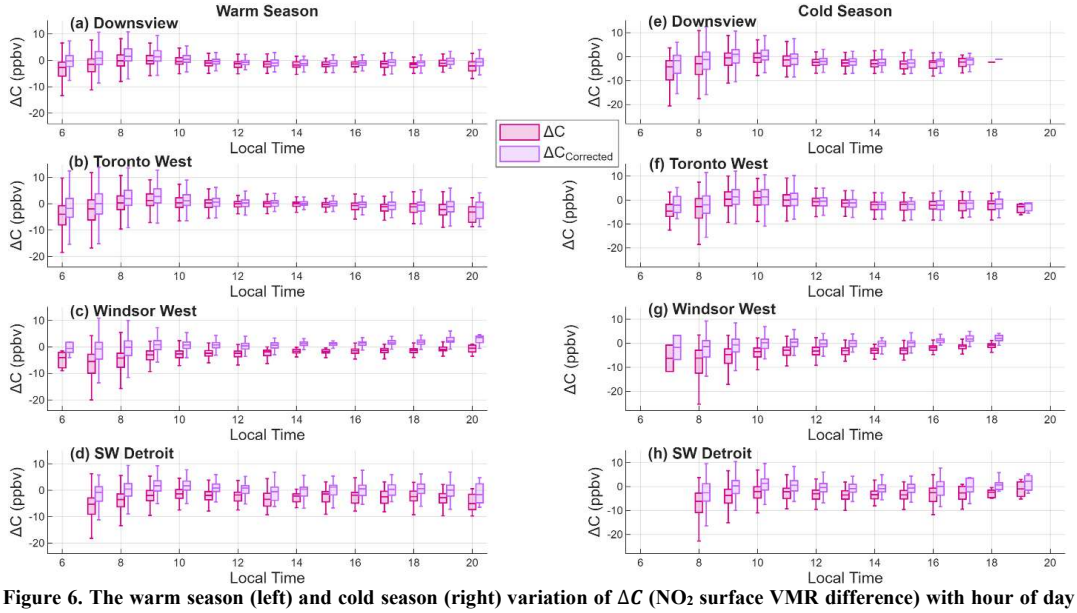


Figure 6. The warm season (left) and cold season (right) variation of ΔC (NO_2 surface VMR difference) with hour of day when the PBL height is below 750 m. The box plots present the hourly ΔC differences for the original Pandora-derived VMRs (red) and $\Delta C_{Corrected}$ for PBL height (purple); they show the median and inter-quartile range while the whiskers show the range of values excluding outliers. Each panel contains data for one site among Downsview (2020-2024), Toronto West (2022-2024), Windsor West (2022-2024), and SW Detroit (2021-2024). Panels (a)-(d) show differences from the beginning of March through the end of August annually. Panels (e)-(f) show differences from the beginning of September through the end of February annually.

https://doi.org/10.5194/egusphere-2026-5916
Preprint. Discussion started: 9 November 2026
© Author(s) 2026. CC BY 4.0 License.

4.2 Wind direction dependence

The difference ΔC varies with meteorological conditions, including wind direction and PBL height. This dependence can explain some of the structure observed in the diurnal and seasonal comparisons. The wind direction results show good agreement between the Pandora-derived surface NO_2 and the in situ measurements when the wind comes from the directions of nearby sources of NO_2. The derived surface VMRs were found to be sensitive to the variation captured by the in situ instruments as a function of wind direction.

Figure 7 shows the NO_2 surface VMR (the in situ measurements and the original and PBL-height-corrected Pandora data) as a function of ERA-5 wind direction at all four sites. The patterns for the in situ and derived NO_2 surface VMRs as a function of wind direction tend to have maxima when the wind is coming from the same direction at a given site, so the Pandora surface estimate is sensitive to the same wind direction dependence as the in situ measurements.

In Fig. 7, the directions are written as degrees clockwise from north, 0° indicating wind coming from the north, 90° indicating wind coming from the east, and so on. In Fig. 7(a), the in situ, derived, and corrected surface VMRs at Downsview indicate that measured NO_2 is larger when the wind is coming from direction of Pearson International Airport, located to the southwest of the site. Fig. 7(b) shows results for Toronto West, for which Highway 401 is located nearby and north of the site, while Pearson International Airport is located to the southwest. The derived values at Toronto West are sometimes larger than the in situ measurements, and it is suspected that when the wind comes from the airport and the PBL height is low, the Pandora direct sun measurements would be sensitive to lofted plumes of NO_2 that are neither measured by the in situ instrument nor accounted for in the GEOS-Chem free tropospheric column. At Windsor West, Fig. 7(c), and SW Detroit, Fig. 7(d), the patterns are very similar, with peaks in all three VMR datasets along the direction from the Zug Island large point source, which corresponds to about 270° at Windsor West and about 250° at SW Detroit.

https://doi.org/10.5194/egusphere-2026-5916
Preprint. Discussion started: 9 November 2026
© Author(s) 2026. CC BY 4.0 License.

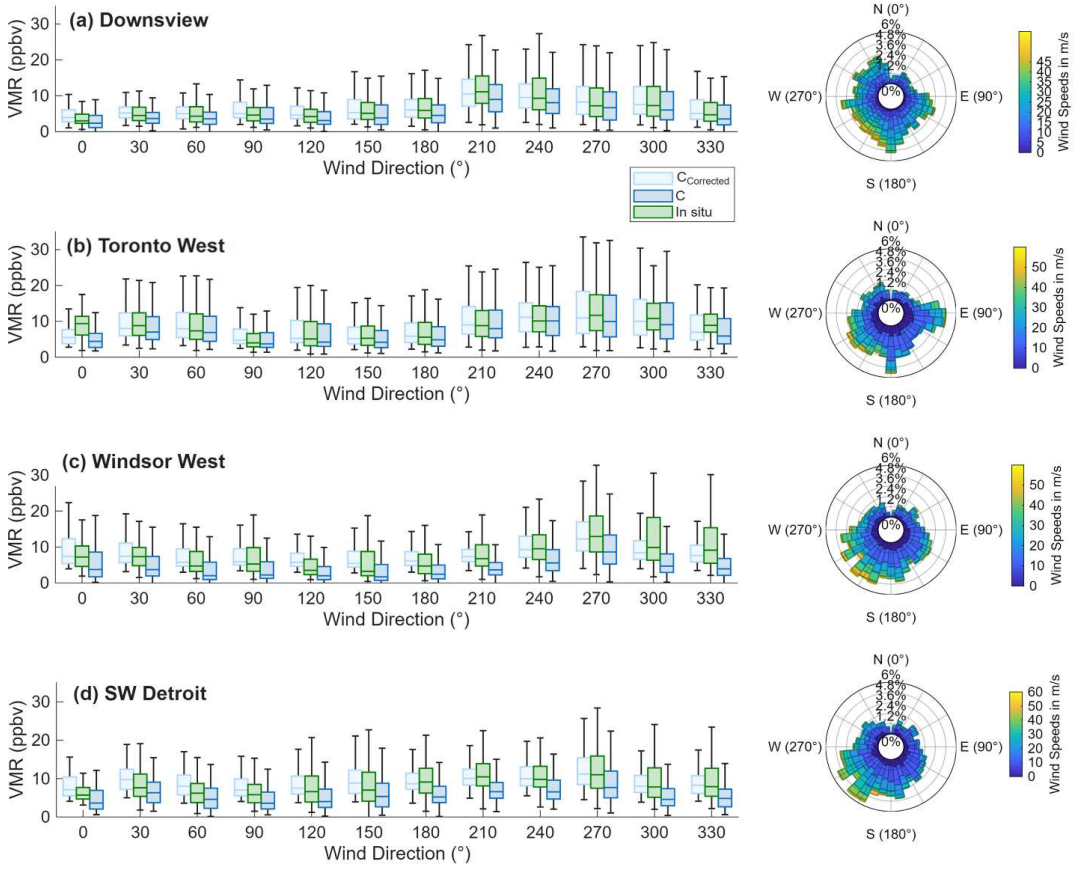


Figure 7. Variation of NO_2 surface VMR with wind direction when the PBL height is below 750 m. Each panel contains data for one site: (a) Downsview, (b) Toronto West, (c) Windsor West, and (d) SW Detroit. $C_{Corrected}$ is calculated based on the PBL dependence of the difference between the original Pandora-derived C and in situ data. In each bin, C corrected (cyan), C (blue), and in situ (green) are shown side by side. Wind direction is binned in 30° increments, with 0° corresponding to wind coming from due north and 90° corresponding to wind coming from due east, so the leftmost trio of box plots represents the data in the bin from 345° through 45° centred on due north. The box plots show the median and inter-quartile range while the whiskers show the range of values excluding outliers. The wind rose plots to the right of each box plot show the relative amount of data from that site coming from each wind direction bin (e.g., wind in the S (180°) bin is approaching the site from the south), colour coded by wind speed.

5 Conclusions

This study set out to determine how effectively the column-to-surface conversion method of Zhao et al. (2019) performs when applied to Pandora direct sun NO_2 total columns at urban sites. NO_2 surface VMRs were derived from Pandora column measurements using GEM-MACH ratios of NO_2 surface VMR to PBL column, Pandora climatological stratospheric NO_2 columns,

https://doi.org/10.5194/egusphere-2026-5916
Preprint. Discussion started: 9 November 2026
© Author(s) 2026. CC BY 4.0 License.

and GEOS-Chem free tropospheric NO_2 columns. The method was applied to Pandora direct sun measurements at four sites: Downsview (2020-2024) and Toronto West (2022-2024) in the Greater Toronto Area, and Windsor West (2022-2024) and SW Detroit (2021-2024) in the Detroit-Windsor Area, all of which had co-located in situ measurements of surface NO_2 that were used to assess how well the derived surface estimates capture surface NO_2 behaviour. The derived VMRs agreed with the coincident in situ measurements to within 2 ppbv over the study period.

There are also operational PGN surface concentrations (S_{conc}) based on MAX-DOAS observations. However, they have not been used in this paper, since they give an estimation of the average S_{conc} along the MAX-DOAS line-of-sight (selected azimuth) of the instrument. The horizontal extent of this average varies with solar zenith angle and aerosol content; it typically ranges from about 5 to 20 km for NO_2 retrieved in the visible range. In contrast, the S_{conc} from direct sun data converted as described in this work are more local, since the direct solar beam passes through the lowest atmospheric layers near the instrument. Several studies have shown that the MAX-DOAS S_{conc} does not agree well with measurements by co-located in-situ sensors at urban sites, but does agree rather well with the average over in-situ sensors distributed along the MAX-DOAS line-of-sight. As the goal of this study is to estimate the local S_{conc} in the best possible way, the DS-based method is preferred to the MAX-DOAS-based method.

The dependence of the results on meteorological conditions was investigated, and it was found that the results are not strongly dependent on temperature. However, the derived NO_2 surface VMRs did exhibit some dependence on PBL height and on wind direction relative to point sources. The method is shown to be most effective when the PBL is above 750 m as estimated by ERA5 reanalysis, with an empirical correction method developed for when the PBL height is below 750 m. The NO_2 surface VMR derived from Pandora direct sun measurements when the PBL is below 750 m has a median difference of -1.7 ppbv (10^{th} percentile: -8.2 ppbv, 90^{th} percentile: 3.2 ppbv) with respect to coincident in situ measurements. When a logarithmic correction is applied as a function of PBL height for these shallow PBL conditions, the median difference is reduced to 0.5 ppbv (-4.8 ppbv, 4.1 ppbv).

Overall, this study demonstrates that Pandora direct sun measurements can be used to derive NO_2 surface VMR at urban sites, with some dependence on PBL height, thus complementing in situ instruments to support long-term monitoring of ambient air quality. The sample size of this study was limited to sites with co-located in situ and Pandora instruments in

https://doi.org/10.5194/egusphere-2026-5916
Preprint. Discussion started: 9 November 2026
© Author(s) 2026. CC BY 4.0 License.

the GTA and DWA. The performance of the algorithm in non-urban environments remains an open question. Future studies could extend the application of this column-to-surface approach to sites with fewer nearby point sources or different meteorological conditions.

Appendix A

The matrix fitting method applied in this work is described by the matrix equations below. Equation (A1) represents how the vector of differences relates to the logarithm of the vector of Planetary Boundary Layer Height (BLH). The $\overrightarrow{\boldsymbol{BLH}}$, $\overrightarrow{\boldsymbol{C}_{pan}}$, and $\overrightarrow{\boldsymbol{C}_{in\ situ}}$ in the equations are vector time series of measurements or model outputs. The logarithm is scaled by parameter a at all sites and shifted by offset parameter b_i for each individual site, represented together as $\vec{\boldsymbol{b}}$ in Eq. (A2). During the matrix fitting, all measurements are used to fit the b_i parameter with equal weighting, while each offset parameter b_i is fitted only using measurements from the relevant site to account for differences in horizontal or vertical location of the in situ and Pandora instruments at a given site.

The $\overrightarrow{\boldsymbol{BLH}}$ in Eq. (A3) is a vector comprising the time series of ERA5 BLH values at each site concatenated vertically such that all data for each site are included in the vector; $\overrightarrow{\boldsymbol{C}_{pan}}$ and $\overrightarrow{\boldsymbol{C}_{in\ situ}}$ are constructed the same way.

The identity matrix **A** is expressed simply in Eq. (A4) and more completely in Eq. (A5); it is a large matrix that locates the indices of $\overrightarrow{\Delta \boldsymbol{C}}$ and $\overrightarrow{\boldsymbol{BLH}}$ corresponding to a given site and is used to expand $\vec{\boldsymbol{b}}$. Equation (A6) represents the same relationship as Eq. (A1) with each of the vectors expressed explicitly.

When applied to the data, the fitting outputs are as shown in Table A1; there is only one value for *a,* and each site has a site-specific value for *b***.** The table also includes the mean and standard deviation of the differences between the in situ and Pandora values after the correction from applying this matrix fitting approach.

$$\overrightarrow{\Delta \boldsymbol{C}} = \overrightarrow{\boldsymbol{C}_{pan}} - \overrightarrow{\boldsymbol{C}_{in\ situ}} = a \log(\overrightarrow{\boldsymbol{BLH}}) + \vec{\boldsymbol{b}} * \mathbf{A} \quad \text{(A1)}$$

$$\vec{\boldsymbol{b}} = \begin{matrix} b_1 \\ \vdots \\ b_4 \end{matrix} \quad \text{(A2)}$$

https://doi.org/10.5194/egusphere-2026-5916
Preprint. Discussion started: 9 November 2026
© Author(s) 2026. CC BY 4.0 License.

$$\overrightarrow{\boldsymbol{BLH}} = \begin{matrix} BLH_1(t_{start}) \\ \vdots \\ BLH_1(t_{end}) \\ BLH_2(t_{start}) \\ \vdots \\ BLH_2(t_{end}) \\ BLH_3(t_{start}) \\ \vdots \\ \vdots \\ BLH_4(t_{end}) \end{matrix} \quad \text{(A3)}$$

$$\mathrm{A}_{ij}(t) = \begin{cases} 1 & i = j \\ 0 & i \neq j \end{cases} \quad \text{(A4)}$$

$$\mathrm{A} = \left[\begin{array}{cccc} \mathrm{A}_{11}(t_{start}) = 1 & \mathrm{A}_{12}(t_{start}) = 0 & \mathrm{A}_{13}(t_{start}) = 0 & \mathrm{A}_{14}(t_{start}) = 0 \\ \vdots & \vdots & \vdots & \vdots \\ \mathrm{A}_{11}(t_{end}) = 1 & \mathrm{A}_{12}(t_{end}) = 0 & \mathrm{A}_{13}(t_{end}) = 0 & \mathrm{A}_{14}(t_{end}) = 0 \\ \hline \mathrm{A}_{21}(t_{start}) = 0 & \mathrm{A}_{22}(t_{start}) = 1 & \mathrm{A}_{23}(t_{start}) = 0 & \mathrm{A}_{24}(t_{start}) = 0 \\ \vdots & \vdots & \vdots & \vdots \\ \mathrm{A}_{21}(t_{end}) = 0 & \mathrm{A}_{22}(t_{end}) = 1 & \mathrm{A}_{23}(t_{end}) = 0 & \mathrm{A}_{24}(t_{end}) = 0 \\ \hline \mathrm{A}_{31}(t_{start}) = 0 & \mathrm{A}_{32}(t_{start}) = 0 & \mathrm{A}_{33}(t_{start}) = 1 & \mathrm{A}_{34}(t_{start}) = 0 \\ \vdots & \vdots & \vdots & \vdots \\ \mathrm{A}_{31}(t_{end}) = 0 & \mathrm{A}_{32}(t_{end}) = 0 & \mathrm{A}_{33}(t_{end}) = 1 & \mathrm{A}_{34}(t_{end}) = 0 \\ \hline \mathrm{A}_{41}(t_{start}) = 0 & \mathrm{A}_{42}(t_{start}) = 0 & \mathrm{A}_{43}(t_{start}) = 0 & \mathrm{A}_{44}(t_{start}) = 1 \\ \vdots & \vdots & \vdots & \vdots \\ \mathrm{A}_{41}(t_{end}) = 0 & \mathrm{A}_{42}(t_{end}) = 0 & \mathrm{A}_{43}(t_{end}) = 0 & \mathrm{A}_{44}(t_{end}) = 1 \end{array}\right] \quad \text{(A5)}$$

$$\begin{matrix} C_{\substack{\text{pan} \\ \text{site 1}}}(t_{\text{start}}) \\ \vdots \\ C_{\substack{\text{pan} \\ \text{site 4}}}(t_{\text{end}}) \end{matrix} - \begin{matrix} C_{\substack{\text{in situ} \\ \text{site 1}}}(t_{\text{start}}) \\ \vdots \\ C_{\substack{\text{in situ} \\ \text{site 4}}}(t_{\text{end}}) \end{matrix} = a \log \begin{pmatrix} BLH_{\text{site 1}}(t_{\text{start}}) \\ \vdots \\ BLH_{\text{site 4}}(t_{\text{end}}) \end{pmatrix} + \begin{matrix} b_1 \\ \vdots \\ b_4 \end{matrix} \mathbf{A} \quad \text{(A6)}$$

Table A1. Table of fitting parameters a and b corresponding to the NO_2 VMR offset between in situ measurements and Pandora DS-derived estimates, that is the difference between the two ($\Delta C_{corrected}$), as best value and uncertainty, and the results of $C_{pan-corrected}$ using the fitted parameters.

Site Name	a [ppbv]	b [ppbv]	$C_{in\ situ}$ Mean (Std Dev) [ppbv]	$C_{pan-corrected}$ Mean (Std Dev) [ppbv]	$\Delta C_{corrected}$ Mean (Std Dev) [ppbv]
Downsview	0.7	-4.4	8.5 (7.1)	8.5 (6.6)	6.7e-05 (4.4)
Toronto West	0.7	-2.1	7.7 (6.4)	7.7 (7.4)	8.2e-05 (5.0)
Windsor West	0.7	-6.5	9.1 (7.3)	9.1 (5.8)	0.14e-05 (3.9)
SW Detroit	0.7	-6.5	10.4 (6.8)	10.4 (5.4)	2.7e-05 (4.3)

https://doi.org/10.5194/egusphere-2026-5916
Preprint. Discussion started: 9 November 2026
© Author(s) 2026. CC BY 4.0 License.

Data availability

Pandora data (L2 direct sun NO_2 total columns) are available from the Pandonia Global Network at https://www.pandonia-global-network.org/home/documents/pgn-data/. The PGN datasets used in this work have DOIs 10.48596/pgn.rnvs3p1-8.SWDetroitMI.P147s1, 10.48596/pgn.rnvs3p1-8.Downsview.P104s1, 10.48596/pgn.rnvs3p1-8.Windsor-West.P208s1, and 10.48596/pgn.rnvs3p1-8.Toronto-West.P108s1. AQS data for criteria gases are available in pre-generated hourly files at https://aqs.epa.gov/aqsweb/airdata/download_files.html. The NAPS in situ data can be downloaded from https://data-donnees.az.ec.gc.ca/data/air/monitor/national-air-pollution-surveillance-naps-program/ (Government of Canada, 2026). ERA5 reanalysis data are available from the Climate Data Service (Copernicus Climate Change Service, 2023a,b). The NO_2 surface volume mixing ratios (ppbv) for all four sites have been compiled into netCDF files along with two of the inputs used in this derivation: (1) the hourly ratios of GEM-MACH surface volume mixing ratio (ppbv) to planetary boundary layer column (molec/cm^2), and (2) GEOS-Chem v8-03-01 free tropospheric columns (molec/cm^2) that have been interpolated from monthly values to hourly timesteps using Pratmo Box model outputs. These datasets are available at https://doi.org/10.5683/SP4/T8OLFY (Bates et al., 2026).

Author contributions

DB, XZ, and KS conceived this project. DB was responsible for conducting the data analysis, creating all the figures, and drafting the paper. XZ, DG, RA, KS, and YS provided input throughout the study and the writing of the manuscript. XZ, VF, and SCL operated and maintained the Pandora instruments in the GTA, and Lukas Valin (LV) and XZ operated and maintained the Pandora instruments in the DWA. DG provided the GEM-MACH data products and GEOS-Chem data products. YS provided the NAPS in situ data. LV provided the AQS in situ data. AC is the PI of the Pandonia Global Network and provided vital technical support for the Downsview site and the ensuing data analysis. All co-authors provided feedback on the paper.

https://doi.org/10.5194/egusphere-2026-5916
Preprint. Discussion started: 9 November 2026
© Author(s) 2026. CC BY 4.0 License.

Competing interests

At least one of the co-authors is a member of the editorial board of *Atmospheric Measurement Techniques*. The authors have no other competing interests to declare.

Acknowledgements

Darby Bates was supported by funding from the University of Toronto Faculty of Arts & Science and the ECCC Grants and Contributions Program (contribution agreement no. GCXE22S069) and would like to express her gratitude for this support. We would like to thank the PIs, support staff, and funding agencies for establishing and maintaining the Pandora 104, 108, 147, and 208 instruments of the Pandonia Global Network used in this investigation. The PGN is a bilateral project supported with funding from NASA and ESA and contributions from EPA, NIER and EUMETSAT. GEOS-Chem and GEM-MACH outputs were provided by ECCC. The deployment of Windsor-West and SW-Detroit Pandora sites are efforts from the Michigan-Ontario Ozone Source Experiment (MOOSE) campaign (Olaguer et al., 2023). We thank MOOSE science team leads Andrew Snider (ECCC) and Jay Olaguer (Michigan EGLE), and MECP and EGLE staff who contributed to in situ NO_2 measurements at the four sites. We also thank Lukas Valin, James Szykman, Eric Baumann, David Williams, and the EPA Office of Research and Development for the SW Detroit Pandora data. We acknowledge the European Centre for Medium-Range Weather Forecasts for providing the ERA5 reanalysis data used in this study, which are publicly available through the Copernicus Climate Change Service.

References

Bates, D., Alwarda, R., Strong, K., Zhao, X., Lee, S. C., Griffin, D., Su, Y., and Cede, A.: Replication Data for: Retrieval of surface NO_2 from Pandora direct sun measurements, Borealis [dataset] https://doi.org/10.5683/SP4/T8OLFY, 2026.

Bey, I., Jacob, D. J., Yantosca, R. M., Logan, J. A., Field, B. D., Fiore, A. M., Li, Q., Liu, H. Y., Mickley, L. J., and Schultz, M. G.: Global modeling of tropospheric chemistry with assimilated meteorology: Model description and evaluation, J. Geophys. Res. Atmos., 106, 23073–23095, https://doi.org/10.1029/2001JD000807, 2001.

https://doi.org/10.5194/egusphere-2026-5916
Preprint. Discussion started: 9 November 2026
© Author(s) 2026. CC BY 4.0 License.

Brohede, S., McLinden, C. A., Urban, J., Haley, C. S., Jonsson, A. I., and Murtagh, D.: Odin stratospheric proxy NO_y measurements and climatology, Atmos. Chem. Phys., 8, 5731–5754, https://doi.org/10.5194/acp-8-5731-2008, 2008.

Brohede, S. M., Haley, C. S., McLinden, C. A., Sioris, C. E., Murtagh, D. P., Petelina, S. V., Llewellyn, E. J., Bazureau, A., Goutail, F., Randall, C. E., Lumpe, J. D., Taha, G., Thomasson, L. W., and Gordley, L. L.: Validation of Odin/OSIRIS stratospheric NO_2 profiles, J. Geophys. Res. Atmos., 112, https://doi.org/10.1029/2006JD007586, 2007.

Canadian Council of Ministers of the Environment: Canadian Ambient Air Quality Standards Handbook, ISBN 978-1-77202-092-2, https://ccme.ca/en/res/caaqshandbook.pdf, 2025.

Cede, A.: Manual for Blick Software Suite 1.8, https://www.pandonia-global-network.org/assets/manuals/BlickSoftwareSuite_Manual_v1-8-6.pdf, 2024.

Cede, A., Tiefengraber, M., Gebetsberger, M., and Spinei Lind, E.: Pandonia Global Network Data Products Readme Document Version 1.8-10, https://www.pandonia-global-network.org/assets/manuals/PGN_DataProducts_Readme_v1-8-10.pdf, 2025.

Copernicus Climate Change Service, Climate Data Store (C3S): ERA5 hourly data on pressure levels from 1940 to present, https://doi.org/10.24381/cds.bd0915c6, 2023a.

Copernicus Climate Change Service, Climate Data Store (C3S): ERA5 hourly data on single levels from 1940 to present, https://doi.org/10.24381/cds.adbb2d47, 2023b.

Di Bernardino, A., Mevi, G., Iannarelli, A. M., Falasca, S., Cede, A., Tiefengraber, M., and Casadio, S.: Temporal Variation of NO_2 and O_3 in Rome (Italy) from Pandora and In Situ Measurements, Atmosphere, 14, 594, https://doi.org/10.3390/atmos14030594, 2023.

Esri. "World Street Map" [basemap]. Scale Not Given. ArcGIS Online, 2026, arcgis.com. Accessed 9 Nov. 2026.

Government of Canada: National Air Pollution Surveillance Program, https://data-donnees.az.ec.gc.ca/data/air/monitor/national-air-pollution-surveillance-naps-program/, 2026.

Judd, L. M., Al-Saadi, J. A., Szykman, J. J., Valin, L. C., Janz, S. J., Kowalewski, M. G., Eskes, H. J., Veefkind, J. P., Cede, A., Mueller, M., Gebetsberger, M., Swap, R., Pierce, R. B., Nowlan, C. R., Abad, G. G., Nehrir, A., and Williams, D.: Evaluating Sentinel-5P TROPOMI tropospheric NO_2 column densities with airborne and Pandora spectrometers near New York City and Long Island Sound, Atmos. Meas. Tech., 13, 6113–6140, https://doi.org/10.5194/amt-13-6113-2020, 2020.

Lamsal, L. N., Duncan, B. N., Yoshida, Y., Krotkov, N. A., Pickering, K. E., Streets, D. G., and Lu, Z.: U.S. NO_2 trends (2005–2013): EPA Air Quality System (AQS) data versus improved observations from the Ozone Monitoring Instrument (OMI), Atmos. Environ., 110, 130–143, https://doi.org/10.1016/j.atmosenv.2015.03.055, 2015.

https://doi.org/10.5194/egusphere-2026-5916
Preprint. Discussion started: 9 November 2026
© Author(s) 2026. CC BY 4.0 License.

Lindenmaier, R., Strong, K., Batchelor, R. L., Bernath, P. F., Chabrillat, S., Chipperfield, M. P., Daffer, W. H., Drummond, J. R., Feng, W., Jonsson, A. I., Kolonjari, F., Manney, G. L., McLinden, C., Ménard, R., and Walker, K. A.: A study of the Arctic NO_y budget above Eureka, Canada, J. Geophys. Res. Atmos., 116, n/a-n/a, https://doi.org/10.1029/2011JD016207, 2011.

McLinden, C. A., Olsen, S. C., Hannegan, B., Wild, O., Prather, M. J., and Sundet, J.: Stratospheric ozone in 3-D models: A simple chemistry and the cross-tropopause flux, J. Geophys. Res. Atmos., 105, 14653–14665, https://doi.org/10.1029/2000JD900124, 2000.

McLinden, C. A., Fioletov, V., Boersma, K. F., Kharol, S. K., Krotkov, N., Lamsal, L., Makar, P. A., Martin, R. V., Veefkind, J. P., and Yang, K.: Improved satellite retrievals of NO_2 and SO_2 over the Canadian oil sands and comparisons with surface measurements, Atmos. Chem. Phys., 14, 3637–3656, https://doi.org/10.5194/acp-14-3637-2014, 2014.

Moran, M. D., Savic-Jovcic, V., Stroud, C. A., Ménard, S., Gong, W., Zhang, J., Zheng, Q., Chen, J., Akingunola, A., Lupu, A., Menelaou, K., and Munoz-Alpizar, R.: Operational chemical weather forecasting with the ECCC online Regional Air Quality Deterministic Prediction System version 023 (RAQDPS023) - Part 1: System description, Geosci. Model Dev., 19, 4137–4203, https://doi.org/10.5194/gmd-19-4137-2026, 2026.

Moran, M. D., Lupu, A., Savic-Jovcic, V., Zhang, J., Zheng, Q., Boutzis, E. I., Mashayekhi, R., Stroud, C. A., Ménard, S., Chen, J., Menelaou, K., Munoz-Alpizar, R., Kornic, D., and Manseau, P. M.: Operational chemical weather forecasting with the ECCC online Regional Air Quality Deterministic Prediction System version 023 (RAQDPS023) - Part 2: Multi-year prospective and retrospective performance evaluation, Geosci. Model Dev., 19, 4205–4270, https://doi.org/10.5194/gmd-19-4205-2026, 2026.

Park, J.-U., Park, J.-S., Diaz, D. S., Gebetsberger, M., Müller, M., Shalaby, L., Tiefengraber, M., Kim, H.-J., Park, S. S., Song, C.-K., and Kim, S.-W.: Spatiotemporal inhomogeneity of total column NO_2 in a polluted urban area inferred from TROPOMI and Pandora intercomparisons, GIScience Remote Sens., 59, 354–373, https://doi.org/10.1080/15481603.2022.2026640, 2022.

Siu, T. K., Goldberg, D. L., Kerr, G. H., Chen, L., Nawaz, M. O., Chang, R. Y.-W., and Fong, K. C.: Tropospheric NO_2 Patterns in Eastern Canada Using the First Year of TEMPO Observations, J. Geophys. Res. Atmos., 130, e2025JD044757, https://doi.org/10.1029/2025JD044757, 2025.

The MathWorks Inc.: MATLAB, version: 25.2.0 (R2025b), Natick, Massachusetts, USA, https://www.mathworks.com, 2025.

The MathWorks Inc.: Mapping Toolbox, version: 25.2 (R2025b), Natick, Massachusetts, USA, https://www.mathworks.com/products/mapping.html, 2025.

Verhoelst, T., Compernolle, S., Pinardi, G., Lambert, J.-C., Eskes, H. J., Eichmann, K.-U., Fjæraa, A. M., Granville, J., Niemeijer, S., Cede, A., Tiefengraber, M., Hendrick, F., Pazmiño, A., Bais, A., Bazureau, A., Boersma, K. F., Bognar, K., Dehn, A., Donner, S., Elokhov, A., Gebetsberger, M., Goutail, F., Grutter de la Mora, M., Gruzdev, A., Gratsea, M., Hansen, G. H., Irie, H., Jepsen, N., Kanaya, Y., Karagkiozidis, D., Kivi, R., Kreher, K., Levelt, P. F., Liu, C., Müller, M., Navarro Comas, M., Piters, A. J. M., Pommereau, J.-P., Portafaix, T., Prados-Roman, C., Puentedura, O.,

https://doi.org/10.5194/egusphere-2026-5916
Preprint. Discussion started: 9 November 2026
© Author(s) 2026. CC BY 4.0 License.



610 Querel, R., Remmers, J., Richter, A., Rimmer, J., Rivera Cárdenas, C., Saavedra de Miguel, L.,
611 Sinyakov, V. P., Stremme, W., Strong, K., Van Roozendael, M., Veefkind, J. P., Wagner, T.,
612 Wittrock, F., Yela González, M., and Zehner, C.: Ground-based validation of the Copernicus
613 Sentinel-5P TROPOMI NO_2; measurements with the NDACC ZSL-DOAS, MAX-DOAS and
614 Pandonia global networks, Atmos. Meas. Tech., 14, 481–510, https://doi.org/10.5194/amt-14-481-
615 2021, 2021.

616 Zhao, X., Griffin, D., Fioletov, V., McLinden, C., Davies, J., Ogyu, A., Lee, S. C., Lupu, A.,
617 Moran, M. D., Cede, A., Tiefengraber, M., and Müller, M.: Retrieval of total column and surface
618 NO_2 from Pandora zenith-sky measurements, Atmos. Chem. Phys., 19, 10619–10642,
619 https://doi.org/10.5194/acp-19-10619-2019, 2019.

620 Zhao, X., Fioletov, V., Alwarda, R., Su, Y., Griffin, D., Weaver, D., Strong, K., Cede, A., Hanisco,
621 T., Tiefengraber, M., McLinden, C., Eskes, H., Davies, J., Ogyu, A., Sit, R., Abboud, I., and Lee,
622 S. C.: Tropospheric and Surface Nitrogen Dioxide Changes in the Greater Toronto Area during
623 the First Two Years of the COVID-19 Pandemic, Remote Sens., 14, 1625,
624 https://doi.org/10.3390/rs14071625, 2022.